

Neutron valence structure from nuclear deep inelastic scattering

E.P. Segarra,¹ A. Schmidt,^{1,2} T. Kutz,^{1,2} D.W. Higinbotham,³
E. Piassetzky,⁴ M. Strikman,⁵ L.B. Weinstein,⁶ and O. Hen^{1,*}

¹*Massachusetts Institute of Technology, Cambridge, Massachusetts 02139, USA*

²*George Washington University, Washington, D.C., 20052, USA*

³*Thomas Jefferson National Accelerator Facility, Newport News, Virginia 23606, USA*

⁴*School of Physics and Astronomy, Tel Aviv University, Tel Aviv 69978, Israel*

⁵*Pennsylvania State University, University Park, PA, 16802, USA*

⁶*Old Dominion University, Norfolk, Virginia 23529, USA*

(Dated: April 23, 2020)

Mechanisms of spin-flavor SU(6) symmetry breaking in Quantum Chromodynamics (QCD) are studied via an extraction of the free neutron structure function from a global analysis of deep inelastic scattering (DIS) data on the proton and on nuclei from $A = 2$ (deuterium) to 208 (lead). Modification of the structure function of nucleons bound in atomic nuclei (known as the EMC effect) are consistently accounted for within the framework of a universal modification of nucleons in short-range correlated (SRC) pairs. Our extracted neutron-to-proton structure function ratio F_2^n/F_2^p becomes constant for $x_B \geq 0.6$, equalling 0.47 ± 0.04 as $x_B \rightarrow 1$, in agreement with theoretical predictions of perturbative QCD and the Dyson Schwinger equation, and in disagreement with predictions of the Scalar Diquark dominance model. We also predict $F_2^{3\text{He}}/F_2^{3\text{H}}$, recently measured, yet unpublished, by the MARATHON collaboration, the nuclear correction function that is needed to extract F_2^n/F_2^p from $F_2^{3\text{He}}/F_2^{3\text{H}}$, and the theoretical uncertainty associated with this extraction.

INTRODUCTION

Almost all the visible mass in the universe comes from the mass of protons and neutrons, and is dynamically generated by the strong interactions of quarks and gluons [1]. These interactions are described by the theory of strong interactions, Quantum Chromodynamics (QCD). While the structure of low-energy QCD largely follows spin-flavor SU(6) symmetry, this symmetry is broken, as evident by the mass difference between the proton and its first excited state, the Delta resonance. The exact symmetry-breaking mechanism is still an open question. This affects our understanding of emergent QCD phenomena such as baryon structure, masses, and magnetic moments [2]. Answering this question is thus one of the main motivations for the ongoing international effort to measure the quark-gluon structure of hadrons.

Different symmetry-breaking mechanisms can be discriminated among experimentally by measuring nucleon structure functions, which are sensitive to the distributions of quarks inside nucleons. Specifically, realistic models of QCD make very different predictions for the relative probability for a single quark to carry all of the momentum of a neutron compared to that of a proton, i.e., the proton to neutron structure function ratio, $F_2^n(x_B, Q^2)/F_2^p(x_B, Q^2)$, as $x_B \rightarrow 1$ (where $x_B = Q^2/2m\nu$ is the fractional quark momenta in the collinear reference frame where the nucleon is fast, Q^2 is the four-momentum transfer squared, m is the nucleon mass, and ν is the energy transfer).

While the proton structure function has been extensively measured, the lack of a free neutron target prevents equivalent measurements of the neutron structure func-

tion, thereby preventing a direct test of QCD symmetry breaking mechanisms.

Here we use measurements of all available structure functions of nuclei (ranging from deuterium to lead) to extract the free neutron structure function, while consistently accounting for the nuclear-medium induced modification of the quark distributions in atomic nuclei. Using data on such a wide span of nuclei provides a large lever arm that allows us to precisely constrain $F_2^n(x_B, Q^2)/F_2^p(x_B, Q^2)$, obtaining new insight into the fundamental structure of QCD.

We find that as x_B approaches unity, $F_2^n(x_B, Q^2)/F_2^p(x_B, Q^2)$ saturates at a value of 0.47 ± 0.04 , giving credence to modern predictions of QCD such as those based on the Dyson Schwinger Equation (0.41 – 0.49) [2] and Perturbative QCD (3/7) [3]. This contrasts with previous extractions that did not include DIS measurements of nuclei heavier than deuterium [4–6] and claimed to support the scalar di-quark (1/4) [7, 8] view of the nucleon.

The large differences between previous extractions of $F_2^n(x_B, Q^2)/F_2^p(x_B, Q^2)$ and those of this work emphasize the need for direct experimental verification. The MARATHON Experiment [9] recently measured $F_2^{3\text{He}}(x_B, Q^2)/F_2^{3\text{H}}(x_B, Q^2)$ with the goal of providing an independent determination of $F_2^n(x_B, Q^2)/F_2^p(x_B, Q^2)$ with minimal sensitivity to nuclear medium effects. This extraction is based on the assumption that such effects should be very similar for ^3He and ^3H , thereby cancelling in their ratio. Using the results of our global analysis, we present predictions for the $F_2^{3\text{He}}(x_B, Q^2)/F_2^{3\text{H}}(x_B, Q^2)$ ratio and the nuclear correction function required to extract $F_2^n(x_B, Q^2)/F_2^p(x_B, Q^2)$ from it. By comparing our

correction function with those of earlier works we quantify the model uncertainty associated with this extraction, which can be as high as $\sim 25\%$ for current realistic models.

UNIVERSAL NUCLEON MODIFICATION AND THE EMC EFFECT

Given the lack of a free neutron target, the modification of the quark-gluon structure of nucleons bound in atomic nuclei, known as the EMC effect, is the main issue preventing a direct extraction of the free neutron structure function from lepton Deep Inelastic Scattering (DIS) measurements of atomic nuclei, see Ref. [10] for a recent review.

We account for the EMC effect in nuclear DIS data by exploiting recent insight to its origin, gained from observations of a correlation between the magnitude of the EMC effect in different nuclei and the relative amount of short-range correlated (SRC) nucleon pairs in those nuclei [10–15].

SRC pairs are predominantly proton-neutron (pn) pairs [16–21]. They have large relative and individual momenta, smaller center-of-mass momenta, and account for 60-70% of the kinetic energy carried by nucleons in the nucleus [18, 22–24]. Therefore, nucleons in such pairs have significant spatial overlap and are far off their mass-shell ($E^2 - p^2 - m^2 < 0$).

These extreme conditions, and the observed correlation between SRC pair abundances and the magnitude of the EMC effect, imply that the EMC effect could be driven primarily by the modification of the structure functions of nucleons in SRC pairs [10–12].

Utilizing scale separation between SRC and uncorrelated (mean-field) nucleons, Ref. [14] modeled the nuclear structure function as having contributions from unmodified uncorrelated nucleons and from modified correlated nucleons in np -SRC pairs:

$$F_2^A = ZF_2^p + NF_2^n + n_{SRC}^A(\Delta F_2^p + \Delta F_2^n), \quad (1)$$

where N and Z are the number of neutrons and protons in the nucleus ($N + Z = A$), n_{SRC}^A is the average number of nucleons in np -SRC pairs, ΔF_2^p and ΔF_2^n are the average differences between the structure functions of free nucleons and nucleons in SRC pairs, and we omitted the explicit x_B and Q^2 dependence of the F_2 structure functions for brevity. This model assumes that both the EMC effect at $0.3 \leq x_B \leq 0.7$ and nucleon-motion effects (which are important at $x_B > 0.7$) are dominated by short-range correlations [15, 25, 26]. Therefore both are approximately proportional to SRC pair abundances and captured by Eq. 1. This model neglects the contribution of pp - and nn -SRC pairs that, due to the predominance of the Tensor interaction at short-distance, are only $\approx 10\%$ of all NN -SRC pairs in both light and

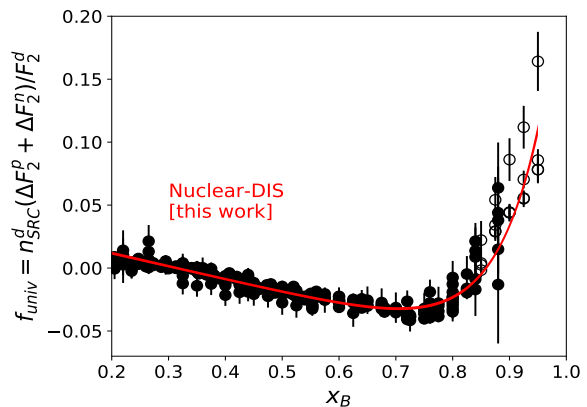


FIG. 1: The extracted global universal modification function (UMF) from the Nuclear-EMC effect analysis performed here (red band). The narrow width of the band shows the 68% confidence interval. Data points show the data-driven extractions of Ref. [14], based on individual measurements of F_2^A/F_2^d in a variety of nuclei. Open and closed data points show measurements at $W < \sqrt{2}$ GeV and $W \geq \sqrt{2}$ GeV respectively.

heavy nuclei [16–21], and have little impact on our results. See supplementary materials for details.

To reduce sensitivity to isospin, target-mass, and higher twist effects [27], DIS data are traditionally given in the form of F_2^A/F_2^d ratios. We use Eq. 1 to express this ratio as:

$$\begin{aligned} \frac{F_2^A}{F_2^d} &= \frac{\Delta F_2^p + \Delta F_2^n}{F_2^d/n_{SRC}^d} \times \left(\frac{n_{SRC}^A}{n_{SRC}^d} - N \right) + (Z - N) \frac{F_2^p}{F_2^d} + N \\ &= f_{\text{univ}}(x_B) \times \left(\frac{n_{SRC}^A}{n_{SRC}^d} - N \right) + (Z - N) \frac{F_2^p}{F_2^d} + N, \end{aligned} \quad (2)$$

where we defined a nucleus independent universal modification function (UMF)

$$f_{\text{univ}} = n_{SRC}^d \frac{\Delta F_2^p + \Delta F_2^n}{F_2^d}. \quad (3)$$

Consistent UMFs were previously extracted for nuclei from ${}^3\text{He}$ to ${}^{208}\text{Pb}$, pointing to the existence of a global UMF for SRC pairs in any nucleus (see Fig. 1) [14]. Here we extract the global UMF using Bayesian inference by means of a Hamiltonian Markov Chain Monte Carlo (HMCMC) [28, 29], referred to herein as Nuclear-DIS analysis.

We parametrized the UMF for all nuclei as

$$f_{\text{univ}} = \alpha + \beta x_B + \gamma e^{\delta(1-x_B)} \quad (4)$$

and estimated its parameters (α , β , γ , and δ) using HMCMC-based inference from F_2^A/F_2^d data [14, 30, 31] for $0.08 \leq x_B \leq 0.95$ in ${}^3\text{He}$, ${}^4\text{He}$, ${}^9\text{Be}$, ${}^{12}\text{C}$, ${}^{27}\text{Al}$, ${}^{56}\text{Fe}$, ${}^{197}\text{Au}$, and ${}^{208}\text{Pb}$, via Eq. 2. Here, and throughout this work, we consistently removed all isoscalar corrections

previously applied to asymmetric nuclei data. We assumed $\frac{n_{SRC}^A/A}{n_{SRC}^d/2} = a_2(A/d)$, the average per-nucleon cross-section ratio for quasi-elastic electron scattering in nucleus A relative to deuterium at $1.5 < x_B < 2$ [12, 14, 32–35]. F_2^p/F_2^d is taken from Table 2 of Ref. [36]. As consistent parameterizations of F_2^p/F_2^d as a function of x_B are needed for the UMF extraction, we parametrized it as $F_2^p/F_2^d = \alpha_d + \beta_d x_B + \gamma_d e^{\delta_d(1-x_B)}$. We determine all parameters, including those of the UMF and F_2^p/F_2^d simultaneously from data as part of the Nuclear-DIS analysis. See online supplementary materials for details on the inference procedure, posterior distributions of the parameters, and discussion of the kinematical coverage of the fitted data.

The Nuclear-DIS analysis reproduced all the F_2^A/F_2^d data over the entire measured x_B range, see online supplementary materials Fig. 1. The resulting global UMF (red band in Fig. 1) extends up to $x_B \sim 0.95$ and agrees well with the individual nuclear UMFs extracted in Ref [14].

F_2^n/F_2^p EXTRACTION

Using Eq. 1 to model nuclear effects in F_2^d we express F_2^n/F_2^p as:

$$\frac{F_2^n}{F_2^p} = \frac{1 - f_{\text{univ}}}{F_2^p/F_2^d} - 1. \quad (5)$$

We extract F_2^n/F_2^p using f_{univ} and F_2^p/F_2^d determined by our Nuclear-DIS analysis discussed above (see Fig. 2). Our results are consistent with the experimental extraction using tagged $d(e, e' p_S)$ DIS measurements on the deuteron [37]. F_2^n/F_2^p decreases steadily for $0.2 \leq x_B < 0.6$, and becomes approximately constant starting at $x_B \approx 0.6$. The $x_B \rightarrow 1$ limit of F_2^n/F_2^p equals 0.47 ± 0.04 .

Removing low- W DIS data ($W < \sqrt{2}$ GeV) from our analysis limits our extraction to $x_B \sim 0.8$ but does not change its conclusions since F_2^n/F_2^p still saturates starting at $x_B \approx 0.6$. The hatched region of the blue band in Fig. 2 corresponds to our model extraction using the low- W DIS data to reach up to $x_B \sim 0.95$. Similarly, we verified that evolving F_2^p/F_2^d from $Q_0^2 = 12$ GeV² to $Q^2 = 5$ GeV² does not significantly change our extraction up to $x_B \sim 0.8$. See online supplementary materials for details.

Our Nuclear-DIS analysis gives significantly larger values of F_2^n/F_2^p than several previous extractions which do not use $A > 2$ nuclear-DIS data, including: (A) CTEQ global analysis (CT14) [4], which uses $W (> 3.5$ GeV) and $Q^2 (> 2$ GeV²) DIS data for $A \leq 2$ (with no corrections for any nuclear effects in the deuteron) combined with various other reactions such as jet production and W^\pm, Z production, (B) CTEQ-JLab global analysis (CJ15) [5], which uses $A \leq 2$ DIS data with looser

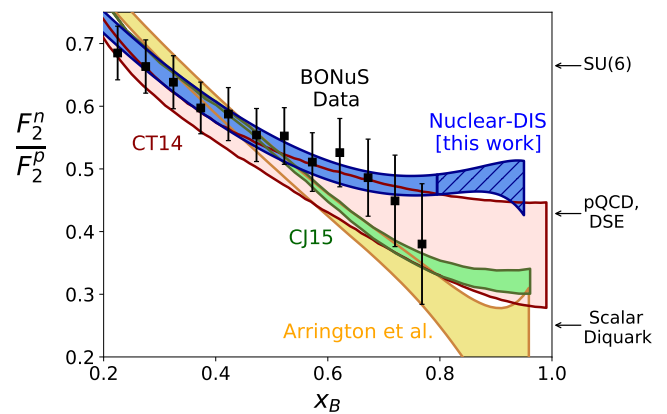


FIG. 2: Neutron-to-proton structure function ratio F_2^n/F_2^p . Data points show the $d(e, e' p_S)$ tagged-DIS measurement [37]. Our predictions (blue band labeled ‘Nuclear-DIS’, including a 68% confidence interval) are compared with those of CT14 [4] (red band), CJ15 [5] (green band), and Arrington et al. [6] (yellow band), which treat nuclear effects in deuteron DIS data differently (see text for details). The labels show F_2^n/F_2^p predictions at $x_B = 1$, such as SU(6) symmetry [39], perturbative QCD (pQCD) [3], Dyson-Schwinger Equation (DSE) [2] and Scalar Diquark models [7, 8]. All predictions are obtained within the parton model framework [27] and all extractions were consistently evolved to the same value of Q^2 based on the kinematics of the MARATHON experiment [9], i.e. $Q^2 = (14 \text{ GeV}^2) \times x_B$.

cuts of $W > 1.7$ GeV and $Q^2 > 1.3$ GeV², together with recently published W^\pm -boson charge asymmetries from D0 [38] and additional corrections for deuteron off-shell, higher-twist, and target-mass effects, and (C) Arrington et al. [6], which includes only $A \leq 2$ DIS data with only corrections for Fermi motion and binding (see Fig. 2).

CT14 and CJ15 extracted parton distribution functions rather than nucleon structure functions. In order to compare their results with our F_2^n/F_2^p extraction, we constructed the corresponding nucleon structure functions from their individual parton distribution functions, accounting for valence region corrections (higher-twist, target-mass) according to Refs. [5, 44]. These corrections largely cancel in the F_2^n/F_2^p ratio.

The comparison with CJ15 is particularly interesting as that extraction of $d(x_B)$ is predominantly constrained by the D0 W^\pm boson asymmetry data [5, 38], corresponding to $Q^2 = m_W^2$. This may indicate a tension between our low Q^2 results and results of the CJ15 analysis of the D0 dataset at $x_B \geq 0.6$.

We find that the $x_B \rightarrow 1$ limit of F_2^n/F_2^p equals 0.47 ± 0.04 for our Nuclear-DIS extraction. Our results agree with predictions based on perturbative QCD [3] and the Dyson-Schwinger Equation (DSE) [2] and disagree with the Scalar Diquark model prediction [7, 8]. This disagrees with the previous extractions (that apply nuclear corrections to the deuteron but do not consis-

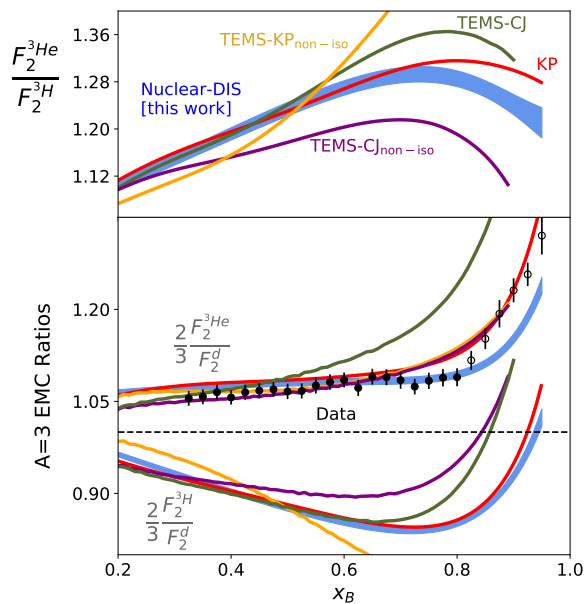


FIG. 3: Top: Nuclear-DIS analysis result for $F_2^{3\text{He}}/F_2^{3\text{H}}$ (blue band) compared to previous extractions by Tropiano et al. [40] (TEMS [green, purple, orange, assuming different off-shell corrections]) and Kulagin and Petti [41, 42] (KP [red]). Bottom: Nuclear-DIS analysis results for $2F_2^{3\text{He}}/3F_2^d$, $2F_2^{3\text{H}}/3F_2^d$ shown in blue. The width of the bands show the 68% confidence intervals of our analysis. Predictions for $2F_2^{3\text{H}}/3F_2^d$ are based on the assumption $n_{SRC}^{3\text{H}} = n_{SRC}^{3\text{He}}$. Symbols show the $2F_2^{3\text{He}}/3F_2^d$ measurement of Ref. [31] re-scaled by $\sim 2\%$. TEMS and KP lines do not include uncertainties. See text for details.

tently use data from heavier nuclei) that either could not discriminate among predictions, or preferred the scalar diquark prediction. Our result is consistent with the upper edge of the CT14 extraction, which does not rely on nuclear corrections. However, our F_2^n/F_2^p has much smaller uncertainties which allow us to discriminate among models.

Thus, accounting for the modification of nucleons bound in deuterium increases F_2^n at high- x_B . This was seen previously, see e.g. Ref. [15, 45–47]. However, the magnitude of this increase at $x_B > 0.6$ is larger in our analysis as compared with those analyses that only use deuterium data. The high- x_B disagreement between our nuclear DIS analysis and the analyses of Refs. [4–6] underscores the need for the forthcoming independent extraction by the MARATHON collaboration. Below we present our predictions for their observables and quantify the model uncertainty associated with their F_2^n/F_2^p extraction.

F_2^n/F_2^p : EXTRACTION FROM $A = 3$ MIRROR-NUCLEI DATA

The MARATHON experiment recently measured DIS on ^2H , ^3H and ^3He . They plan to independently extract F_2^n/F_2^p from $F_2^{3\text{He}}/F_2^{3\text{H}}$ using [9]:

$$\frac{F_2^n}{F_2^p} = \frac{2\mathcal{R} - F_2^{3\text{He}}/F_2^{3\text{H}}}{2F_2^{3\text{He}}/F_2^{3\text{H}} - \mathcal{R}}, \quad (6)$$

where \mathcal{R} is a theoretical correction factor which measures the cancellation of nuclear effects in $F_2^{3\text{He}}/F_2^{3\text{H}}$,

$$\mathcal{R} \equiv \frac{F_2^{3\text{He}}}{2F_2^p + F_2^n} \times \frac{F_2^p + 2F_2^n}{F_2^{3\text{H}}}. \quad (7)$$

Since ^3He and ^3H should have similar nuclear effects \mathcal{R} should be close to 1.

We use our UMF to predict the expected DIS ratios for $[F_2^{3\text{He}}/3]/[F_2^d/2]$, $[F_2^{3\text{H}}/3]/[F_2^d/2]$, and $F_2^{3\text{He}}/F_2^{3\text{H}}$ (see Fig. 3). Since the $n_{SRC}^{3\text{H}}/n_{SRC}^{3\text{He}}$ data are not yet published, we assumed $n_{SRC}^{3\text{H}} = n_{SRC}^{3\text{He}}$. Varying this by $\pm 20\%$ changed our results by less than 5% at moderate and high- x , see online supplementary materials.

We compare our predictions for $[F_2^{3\text{He}}/3]/[F_2^d/2]$, $[F_2^{3\text{H}}/3]/[F_2^d/2]$, and $F_2^{3\text{He}}/F_2^{3\text{H}}$ with other models, shown as colored lines in Fig. 3. Our prediction is overall similar to that of Kulagin and Petti (KP) [41, 42], though there are differences at high x_B in the $[F_2^{3\text{He}}/3]/[F_2^d/2]$, and $F_2^{3\text{He}}/F_2^{3\text{H}}$ ratios. The Tropiano et al. (TEMS) analysis [40] combine the CJ15 global PDF fits [5] and their off-shell correction in deuterium, with additional fits to $[F_2^{3\text{He}}/3]/[F_2^d/2]$ data [31], to extract off-shell corrections in $A = 3$ nuclei. TEMS-CJ assumes fully isoscalar off-shell corrections. In [40], fits allowing non-isoscalar off-shell corrections were also performed, which required an isoscalar correction as input. TEMS-CJ_{non-iso} uses the isoscalar correction from CJ15, while TEMS-KP_{non-iso} uses a different isoscalar correction, developed by Kulagin and Petti [41, 42]. For $x_B > 0.6$, TEMS-CJ_{non-iso} and TEMS-KP_{non-iso} predictions [40] individually disagree with our prediction of $F_2^{3\text{He}}/F_2^{3\text{H}}$. However, the spread of the two curves at $x_B > 0.6$ highlights the minimal sensitivity that $[F_2^{3\text{He}}/3]/[F_2^d/2]$ alone can provide to constraining non-isoscalar off-shell effects. We agree with the isoscalar off-shell predictions of TEMS-CJ up to $x_B \sim 0.5$. For $x_B < 0.5$, even including uncertainty of TEMS-CJ_{non-iso} and TEMS-KP_{non-iso} (see supplementary materials), we predict a slightly higher ratio as compared to these two predictions.

We also studied the effect of different models of \mathcal{R} on the extractions of F_2^n/F_2^p from $F_2^{3\text{He}}/F_2^{3\text{H}}$. Fig. 4 (left panel) shows several theoretical predictions of \mathcal{R} . While individual models vary by only a few percent, the choice of model can lead to significant, differences in the extracted F_2^n/F_2^p , especially at large x_B . Fig. 4 (right

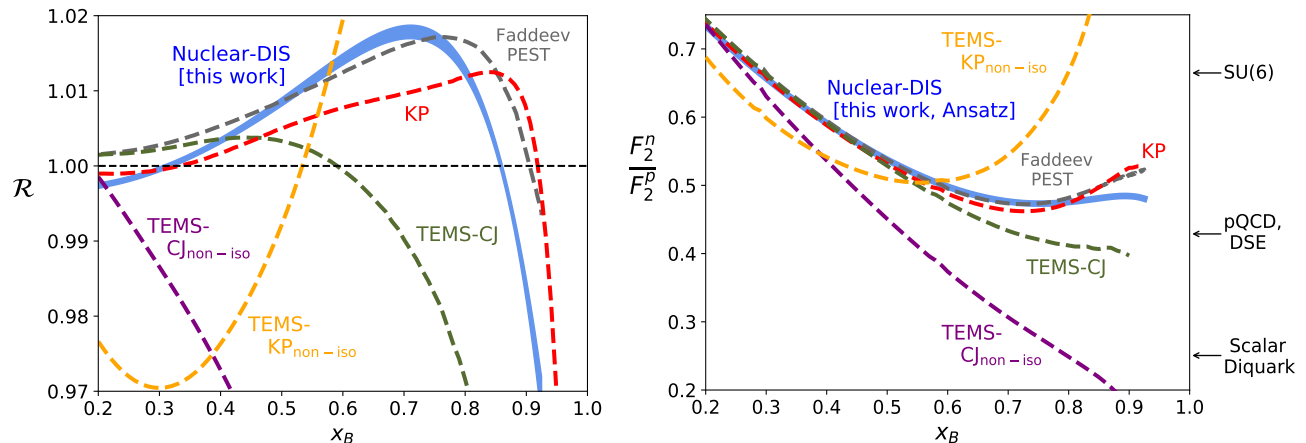


FIG. 4: Left: Different model predictions for \mathcal{R} as defined in Eq. 7. The present work (blue band, labeled ‘Nuclear-DIS’) includes a 68% confidence interval. The other labeled lines show calculations (not including uncertainties) by Tropiano et al. [40] (TEMS, for different off-shell corrections), Kulagin and Petti [41, 42] (KP), and Afnan et al. [43] (Faddeev PEST). Right: F_2^n/F_2^p extracted from predicted values of $F_2^{3\text{He}}/F_2^{3\text{H}}$ using this work (see blue bands in Fig. 3) in combination with different theoretical predictions for \mathcal{R} (see Eq. 6). The blue line here is the central value of the blue band in Fig. 2. See text for details.

panel) shows F_2^n/F_2^p extracted using Eq. 6. Here we assume $F_2^{3\text{He}}/F_2^{3\text{H}}$ from our Nuclear-DIS analysis and then use various models of \mathcal{R} to extract F_2^n/F_2^p , similar to the extraction MARATHON will perform with their measured $F_2^{3\text{He}}/F_2^{3\text{H}}$. While our prediction for $F_2^{3\text{He}}/F_2^{3\text{H}}$ is similar to that of KP (see Fig. 3), the differences at $x_B > 0.7$ create large differences in \mathcal{R} , which cause a $\sim 10\%$ difference in the extracted F_2^n/F_2^p . The predictions of TEMS [40] lead to larger differences in F_2^n/F_2^p and therefore even larger model uncertainties at large- x_B [48]. Performing the extraction of F_2^n/F_2^p with different models for $F_2^{3\text{He}}/F_2^{3\text{H}}$ give similar uncertainty in F_2^n/F_2^p ; see supplementary materials Fig 7.

Once the MARATHON $F_2^{3\text{He}}/F_2^{3\text{H}}$ data is published, this model uncertainty could be reduced by iteratively improving the extracted F_2^n using Eqs. 6 and 7 [9]. However, in this procedure, care must be taken to ensure consistency with global nuclear DIS data, as was done in our analysis.

CONCLUSIONS

Using Bayesian inference by means of a Hamiltonian Markov Chain Monte Carlo, we extracted a nucleon universal modification function (UMF) that is consistent with DIS measurements of nuclei from $A = 2$ to 208. We used it to correct Deuteron DIS data for bound-nucleon structure-modification effects and to extract F_2^n/F_2^p up to $x_B \approx 0.9$.

The extracted F_2^n/F_2^p ratio saturates at high- x_B at a value of 0.47 ± 0.04 , which is consistent with perturbative QCD and DSE predictions [2, 3], is lower than the

SU(6) symmetry prediction of $2/3$ [39], and is significantly greater than the Scalar Diquark model prediction of $1/4$ [7, 8]. Our Nuclear-DIS analysis prediction also agrees with the most recent experimental extraction by the BONuS experiment [37]. The BONuS experiment will take more data soon at higher energies and provide a more stringent test of our predictions. The forthcoming parity-violating DIS program using SoLID at Jefferson Lab will further probe d/u directly using a proton target [49].

We also used the UMF to predict the Tritium and ^3He DIS cross section ratios, recently measured by the MARATHON experiment [9], and to estimate the nuclear correction function \mathcal{R} that they plan to use to extract F_2^n/F_2^p from their data. We showed that different models of \mathcal{R} lead to non-negligible model uncertainty in the planned extraction of F_2^n/F_2^p .

We thank C. Keppel, W. Melnitchouk, and N. Sato for useful discussions. This work was supported by the U.S. Department of Energy, Office of Science, Office of Nuclear Physics under Award Numbers DE-FG02-94ER40818, DE-FG02-96ER-40960, DE-FG02-93ER40771, and DE-AC05-06OR23177 under which Jefferson Science Associates operates the Thomas Jefferson National Accelerator Facility, the Pazy foundation, and the Israeli Science Foundation (Israel) under Grants Nos. 136/12 and 1334/16.

* Contact Author hen@mit.edu

[1] A. Bashir, L. Chang, I. Cloet, B. El-Bennich, Y. Liu, C. Roberts, and P. Tandy, Commun. Theor. Phys. **58**,

- 79 (2012), 1201.3366.
- [2] C. D. Roberts, R. J. Holt, and S. M. Schmidt, Phys. Lett. **B727**, 249 (2013), 1308.1236.
- [3] G. R. Farrar and D. R. Jackson, Phys. Rev. Lett. **35**, 1416 (1975).
- [4] S. Dulat, T.-J. Hou, J. Gao, M. Guzzi, J. Huston, P. Nadolsky, J. Pumplin, C. Schmidt, D. Stump, and C. P. Yuan, Phys. Rev. **D93**, 033006 (2016), 1506.07443.
- [5] A. Accardi, L. T. Brady, W. Melnitchouk, J. F. Owens, and N. Sato, Phys. Rev. **D93**, 114017 (2016), 1602.03154.
- [6] J. Arrington, J. G. Rubin, and W. Melnitchouk, Phys. Rev. Lett. **108**, 252001 (2012), 1110.3362.
- [7] F. E. Close, Phys. Lett. **43B**, 422 (1973).
- [8] R. D. Carlitz, Phys. Lett. **58B**, 345 (1975).
- [9] G. G. Petratos et al., Jefferson Lab PAC37 Proposal (2010), experiment E12-10-103.
- [10] O. Hen, G. A. Miller, E. Piasetzky, and L. B. Weinstein, Rev. Mod. Phys. **89**, 045002 (2017).
- [11] L. B. Weinstein, E. Piasetzky, D. W. Higinbotham, J. Gomez, O. Hen, and R. Shneor, Phys. Rev. Lett. **106**, 052301 (2011).
- [12] O. Hen, E. Piasetzky, and L. B. Weinstein, Phys. Rev. C **85**, 047301 (2012).
- [13] O. Hen, D. W. Higinbotham, G. A. Miller, E. Piasetzky, and L. B. Weinstein, Int. J. Mod. Phys. **E22**, 1330017 (2013), 1304.2813.
- [14] B. Schmookler et al. (CLAS), Nature **566**, 354 (2019).
- [15] L. Frankfurt and M. Strikman, Phys. Rep. **160**, 235 (1988).
- [16] E. Piasetzky, M. Sargsian, L. Frankfurt, M. Strikman, and J. W. Watson, Phys. Rev. Lett. **97**, 162504 (2006).
- [17] R. Subedi et al., Science **320**, 1476 (2008).
- [18] I. Korover, N. Muangma, O. Hen, et al., Phys.Rev.Lett. **113**, 022501 (2014).
- [19] O. Hen et al. (CLAS Collaboration), Science **346**, 614 (2014).
- [20] M. Duer et al. (CLAS), Nature **560**, 617 (2018).
- [21] M. Duer et al. (CLAS), Phys. Rev. Lett. **122**, 172502 (2019), 1810.05343.
- [22] A. Tang et al., Phys. Rev. Lett. **90**, 042301 (2003).
- [23] R. Shneor et al., Phys. Rev. Lett. **99**, 072501 (2007).
- [24] E. O. Cohen et al. (CLAS), Phys. Rev. Lett. **121**, 092501 (2018), 1805.01981.
- [25] M. M. Sargsian et al., J. Phys. **G29**, R1 (2003).
- [26] W. Melnitchouk, M. Sargsian, and M. Strikman, Z. Phys. **A359**, 99 (1997).
- [27] M. Virchaux and A. Milsztajn, Phys. Lett. **B274**, 221 (1992).
- [28] B. Carpenter, A. Gelman, M. Hoffman, D. Lee, B. Goodrich, M. Betancourt, M. Brubaker, J. Guo, P. Li, and A. Riddell, Journal of Statistical Software, Articles **76**, 1 (2017), ISSN 1548-7660, URL <https://www.jstatsoft.org/v076/i01>.
- [29] S. D. Team, *Pystan: the python interface to stan, version 2.17.1.0*, <http://mc-stan.org> (2018).
- [30] J. Gomez et al., Phys. Rev. D **49**, 4348 (1994).
- [31] J. Seely et al., Phys. Rev. Lett. **103**, 202301 (2009).
- [32] L. Frankfurt, M. Strikman, D. Day, and M. Sargsyan, Phys. Rev. C **48**, 2451 (1993).
- [33] K. Egiyan et al. (CLAS Collaboration), Phys. Rev. C **68**, 014313 (2003).
- [34] K. Egiyan et al. (CLAS Collaboration), Phys. Rev. Lett. **96**, 082501 (2006).
- [35] N. Fomin et al., Phys. Rev. Lett. **108**, 092502 (2012).
- [36] J. Arrington, F. Coester, R. J. Holt, and T. S. H. Lee, J. Phys. **G36**, 025005 (2009), 0805.3116.
- [37] N. Baillie et al. (CLAS), Phys. Rev. Lett. **108**, 142001 (2012), [Erratum: Phys. Rev. Lett.108,199902(2012)], 1110.2770.
- [38] V. M. Abazov et al. (D0), Phys. Rev. **D91**, 032007 (2015), [Erratum: Phys. Rev.D91,no.7,079901(2015)], 1412.2862.
- [39] F. E. Close, *An Introduction to Quarks and Partons* (Academic Press, London, 1979).
- [40] A. Tropicano, J. Ethier, W. Melnitchouk, and N. Sato, Phys. Rev. **C99**, 035201 (2019), 1811.07668.
- [41] S. A. Kulagin and R. Petti (private communication).
- [42] S. A. Kulagin and R. Petti, Phys. Rev. **C82**, 054614 (2010), 1004.3062.
- [43] I. R. Afnan, F. R. P. Bissey, J. Gomez, A. T. Katramatou, S. Liuti, W. Melnitchouk, G. G. Petratos, and A. W. Thomas, Phys. Rev. **C68**, 035201 (2003), nucl-th/0306054.
- [44] A. Accardi (private communication).
- [45] W. Melnitchouk and A. W. Thomas, Phys. Lett. **B377**, 11 (1996), nucl-th/9602038.
- [46] U.-K. Yang and A. Bodek, Phys. Rev. Lett. **82**, 2467 (1999), hep-ph/9809480.
- [47] O. Hen, A. Accardi, W. Melnitchouk, and E. Piasetzky, Phys. Rev. D **84**, 117501 (2011).
- [48] M. M. Sargsian, S. Simula, and M. I. Strikman, Phys. Rev. **C66**, 024001 (2002), nucl-th/0105052.
- [49] SoLID Collaboration, <https://hallaweb.jlab.org/12GeV/SoLID/download/doc/SoLIDWhitePaper-Sep9-2014.pdf> (2014).